

Initial formation and evolution of channel-shoal patterns in estuaries

A. Hibma¹, H.M. Schuttelaars^{1,2} and H.J. de Vriend¹

ABSTRACT: A complex process-based model is used to simulate the formation of channels and shoals in a schematised estuary. The model set-up enables a comparison with idealised models. Initial as well as long-term simulations are made. The dominant wavelengths of the channel-shoal patterns are investigated together with the dependency on the width and depth of the basin. The initial model results are compared with idealised models. The prevalent wavelength between 5 and 10 km in the complex model agrees with the length scales found in the idealised model of Schramkowski et al. (2002). Also the growth rates of the amplitudes of the initial perturbations are of the same order of magnitude in both models. A qualitative agreement in dependency on width-depth ratios is found between the complex model and different idealised models. The growth of the perturbations during the long-term simulations gives information on the validity limits of the idealised models. Subsequent pattern formation and changes of the dominant wavelength are attributed to non-linear interactions. At the end of the long-term simulations, the channel-shoal pattern has evolved into a unique morphodynamic equilibrium state, independent of the initial perturbation. This complex model forms a new step in an integrated model approach in which different model types and field data are combined in order to make optimum use of each research method.

1 INTRODUCTION

Estuaries attract a variety of human activities, such as navigation, recreation, fishing, sand mining, land reclamation and in some cases hydrocarbon mining. On the other hand, many estuaries form the basis of highly valuable and sometimes unique ecosystems. They function as nursing, resting and feeding grounds for many species. The interests of the various functions of an estuary can be in mutual conflict. From a management point of view it is important to predict the morphological response of these systems to human activities or changes in environmental conditions. Channels and shoals form highly dynamical elements in estuaries. At this moment, the predictive capability of their morphological behaviour is rather limited. Research on this subject uses different types of models, each giving insight into a certain aspect of the morphodynamics (de Vriend, 1996; de Vriend and Ribberink, 1996). In this contribution we will work with two types of models: idealised and complex models.

In a previous study (Hibma et al., 2003a) it was shown that a complex process-based model of estuarine morphodynamics produces channel and shoal patterns that resemble those observed in nature. Figure 1 shows a result from this study for an initial and an advanced stage of the channel-shoal formation. The patterns exhibit a characteristic wavelength in the longitudinal direction, which increases during the simulation until a relatively stable pattern is established. The mechanisms behind the formation of these channel-shoal patterns and the factors determining the dominant wavelength are difficult to extract from the complex model. To increase the insight into the morphological behaviour, use can be made of idealised models. This type of model makes use of simplifications in model formulations and geometry, in such a way that the prevailing morphological processes can be analysed (Seminara and Tubino,

¹ Delft University of Technology. Faculty of Civil Engineering and Geoscience. P.O. Box 5048. 2600 GA Delft, The Netherlands. A.Hibma@ct.tudelft.nl

² Institute for Marine and Atmospheric research Utrecht (IMAU), Utrecht University, The Netherlands.

1998; 2001; Schuttelaars and de Swart, 1999; Schramkowski et al., 2002). However, these models are restricted to initial linear growth of channel-shoal patterns in idealised situations. An integrated approach, combining these two types of model and confronting them with field observations, can improve the insight into the processes and validate the models.

In this paper we focus on the growth of the channel-shoal patterns of variable wavelength. The dependency on width and depth of the basin and the pattern modification due to non-linear interactions between bathymetry and physical processes are shown. The initial formation is compared with idealised models, which provides insight into the processes in the complex model and the validity of the assumptions underlying linearised models. This forms a new step in the integrated model approach.

In the next section the model approach is described, providing background for the model assumptions, the model set-up and the simulations carried out. Subsequently, the results of the complex model are analysed. In the discussion the initial growth is compared to idealised model results and the transition from initial to strongly non-linear pattern formation is discussed. In the final section conclusions are drawn.

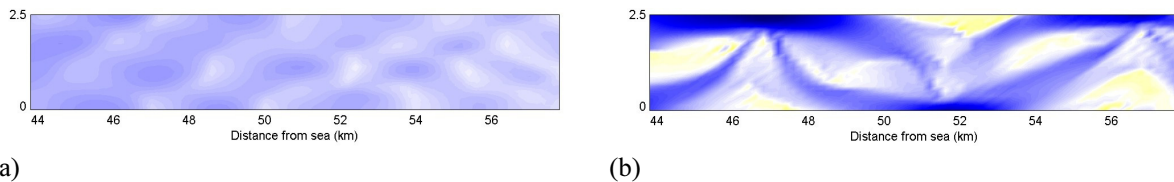


Figure 1: Channel-shoal pattern after (a) 16 years and (b) 110 years of model simulation, starting from a linear sloping bottom profile on which small random perturbations are applied. Fourier analyses show that the dominant wavelength after 16 years is 3.5 km with an amplitude of 1.0 m, and 10 km with an amplitude of 11 m after 110 years.

2 MODEL APPROACH AND ANALYSIS

MODEL APPROACH

In this study the complex process-based model Delft3D (Wang et al., 1991; 1995; Roelvink and Van Banning, 1994) is used to simulate the formation of channels and shoals in an estuary. The model system describes the water motion by the shallow water equations. In this study, the 2-D depth-averaged version of the model is used, as 3D-effects are not required for the pattern formation (Coeveld et al., 2003). The sediment transport can be described by a bed-load or total-load transport formula (using a variety of semi-empirical formulae), or by a quasi-three-dimensional advection-diffusion solver for suspended sediment, including temporal and spatial lag-effects. The bathymetry changes due to divergence or convergence of the sediment flux field.

For a comparison of the initial pattern formation resulting from the complex model with the results of the idealised model, it is essential that the physical formulations in both models be as similar as possible. In an earlier study (Hibma et al., 2003a), it was concluded that mutual validation of results from idealised and complex process-based models is difficult due to the different model assumptions and formulations. In Hibma et al. (2003b), the complex model was adapted such that a comparison of the width-averaged velocities, concentrations and bed profiles was possible for estuaries of arbitrary length. It was concluded that the adaptations

and remaining differences in model formulations have no qualitative influence on the model results, except for the boundary condition of the bed at the entrance of the estuary. In the present study, model settings are adopted from this one-dimensional model. In this way, it can be assumed that the remaining differences in model formulations between the two model types do not obstruct a comparison of results. In accordance with the one-dimensional model, the sediment transport is calculated using an advection-diffusion model. The landward and lateral boundaries are non-erodible. For the time being, the bed level at the seaward open boundary is not fixed. This condition influences primarily the long-term equilibrium profile and is of minor importance to the initial formation for which the comparison with the idealised models is made.

To compare the results with the idealised two-dimensional models, the geometry of the estuary is schematised to a rectangular basin (see Fig. 2). The bed level linearly decreases from the seaward to the landward boundary of the basin. The simulations are made on a grid with a mesh size 125 m x 125 m.

Contrary to the model of Hibma et al. (2003a), the linear sloping bottom profile is not perturbed randomly, but with sinusoidal undulations. This facilitates the investigation of growth rates of patterns of a certain wavelength. These periodic perturbations are described by

$$h'(x, y) = A \sin\left(\frac{2\pi}{\lambda_L} x\right) \cos\left(\frac{2\pi}{\lambda_T} y\right)$$

in which A is the amplitude, λ_L is the wavelength in longitudinal direction and λ_T is the wavelength in transversal direction. In this paper only the first mode, i.e. $\lambda_T = 2B$ is considered.

ANALYSIS OF MODEL RESULTS

In the analysis of the model results the growth rates of these perturbations are studied. The growth rates represent the increase of the amplitude of the perturbation and are presented as a yearly value in order to get a meaningful magnitude. Fourier analysis is applied to determine the evolution of the amplitude of each perturbation during the simulation. Negative growth rates indicate decay of the amplitudes, positive growth rates indicate amplification. The largest growth rate among different perturbations indicates the fastest growing or prevalent wavelength of the channel-shoal pattern formation. A morphological equilibrium is expected to be reached, when the amplitudes of all perturbations have ceased to change.

In the idealised models, the perturbations are regarded as local, i.e. the mean bed level is assumed locally horizontal and in equilibrium. In the complex model a constant bed level is approximated by analysing the results for a short section of the basin. The mean profile underlying the perturbations shows small adjustments during the initial period, which is an order of magnitude smaller than the bed level changes induced by the perturbations. This adaptation of the underlying profile is subtracted from the model results. In this case a Fourier analysis gives the growth rates and prevalent wavelengths of the perturbations, which can be compared with those from the idealised models.

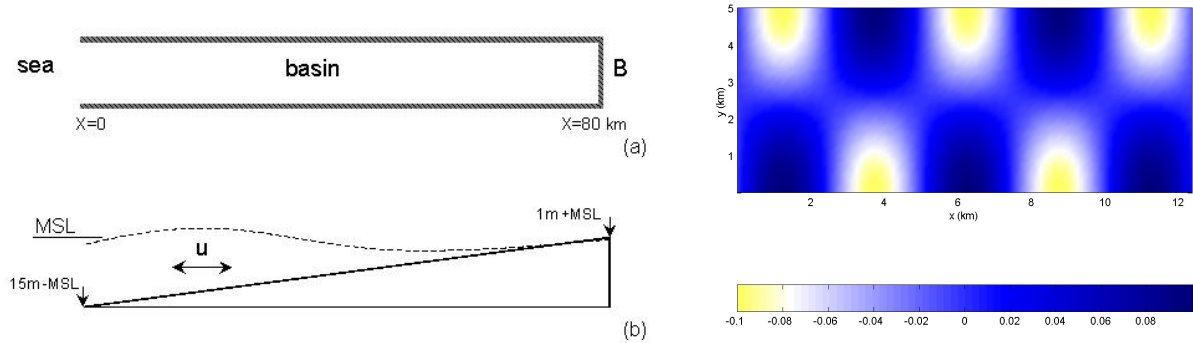


Figure 2. (a) Top view and (b) side view of idealised estuary. (c) Imposed perturbation h' .

3 MODEL EXPERIMENTS

Most physical parameters used in this study are derived from the dynamic seaward part of the Western Scheldt estuary. The width of the modelled basin is 5000 m. Hibma et al. (2003a) showed that the width and depth of the basin influence the prevalent wavelength. To study the influence of the width, also a small basin for which the width is decreased to 500 m is simulated. Both basins are 80 km long and start from a linear sloping bed level. The bottom level decreases from 15 m below MSL at the seaward end to 1 m above MSL at the landward boundary. The bed material consist of uniform sand with a grain size of 200 μm . At the seaward boundary a periodic water level variation is imposed, simulating the M_2 tidal component with an amplitude of 1.75 m. For the bottom roughness a constant Chézy coefficient of 50 $\text{m}^{1/2}/\text{s}$ is used and in the sediment transport a dispersion coefficient of 10 m^2/s is used.

Five perturbations with different wavelengths are imposed on the bed level of the basin. The wavelength of these perturbations is 1, 2, 5, 10 and 15 km in longitudinal direction (λ_L), hereafter referred to as λ_1 to λ_{15} , respectively. The amplitude of the perturbations is 0.1 m. The transversal wavelength (λ_T) is two times the basin width, which means that the perturbations form an alternating pattern. This is labelled as the first mode in the idealised models.

Long-term as well as a short-term simulations are made, for the small and wide basin and with the various perturbations. The short-term simulations are computations during one tidal cycle. The change in amplitude of the perturbations after this cycle is regarded as the initial growth or decay. The results are presented in the next paragraph. These changes take place in the linear domain and will be compared to idealised models, as described in the discussion. Long-term simulations are made for about 100 years. In this period non-linear interactions are playing a dominant role. The results of the long-term simulations are analysed to demonstrate the pattern transformation due to these non-linear interactions and to define the range of linear processes. The results are described hereafter and discussed in the following section.

INITIAL MODEL RESULTS

Figure 3 shows the growth rates along the basins for the different values of the wavelength of the perturbation. The growth rates vary along the basin. The wavelength corresponding to the largest growth rate varies along the estuary.

In the wide basin (Fig. 3a) perturbation λ_{10} is the prevalent wavelength from the seaward boundary to halfway up the basin. Landwards of this point, there is an area where perturbation λ_5 is more unstable. The growth rates of λ_5 show more variation along the basin than those of

the larger perturbations λ_{15} and λ_{10} . They decrease with increasing water depth and become negative at the seaward end of the basin. The smaller perturbations λ_1 and λ_2 have negative growth rates everywhere in this basin. The negative growth rates of λ_1 fall outside the range plotted here.

Fig. 3b shows that perturbation λ_5 is the fastest growing undulation over the major part of the narrow basin. At the landward end, the smaller wavelength λ_2 is the most unstable, at the seaward end larger wavelengths are prevalent. It is observed that the growth rates become smaller as the water depth increases and can even become negative (i.e. λ_2). Also in this narrow basin, perturbation λ_1 has negative growth rates outside the plotted range.

As compared to the narrow basin, the most unstable wavelengths are larger in the wide estuary. The growth rates show less variation along the basin, which indicates that the influence of local depth on the growth is smaller in the wide basin.

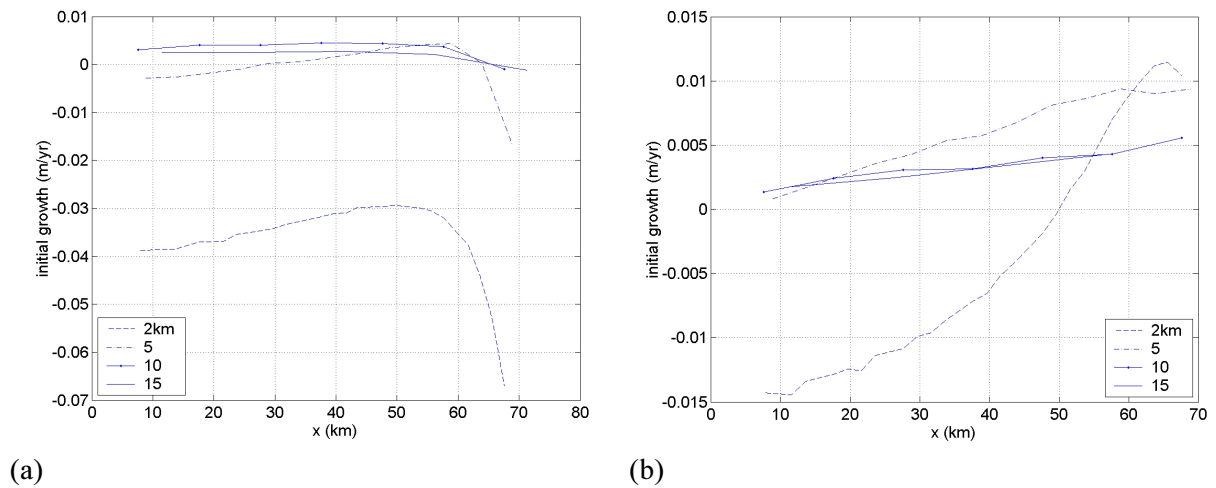


Figure 3. Initial growth of perturbations along the basin in (a) wide basin of 5 km width and (b) narrow basin of 500 m width.

LONG-TERM MODEL RESULTS

In the long-term model simulation for the wide basin the pattern imposed by the initial perturbations gradually changes in amplitude and wavelength. Furthermore, migration can be observed. Figure 4 shows the amplitude evolution of the imposed perturbations during 150 years. The results are given for a section around $x = 50$ km. Fig. 3 shows that at this location λ_{10} is the fastest growing perturbation and that λ_1 and λ_2 are damped. This is also observed in Fig. 4 for the first years of the long-term simulation, where the amplitude of λ_{10} increases fastest. However, after approximately 45 years the amplitude of λ_5 exceeds the amplitude of λ_{10} . During the rest of the simulation, λ_5 remains the dominant wavelength, at least of the ones considered. The amplitude increases during the first 110 years, after which it more or less stabilises. This indicates that the evolving pattern approaches an equilibrium state. Also the ever slower evolution of the overall pattern (not shown) during the last period of the simulation suggest that the system tends towards a more or less static equilibrium. The dominant wavelength of this overall channel-shoal pattern lies between 5 and 10 km in most of the estuary.

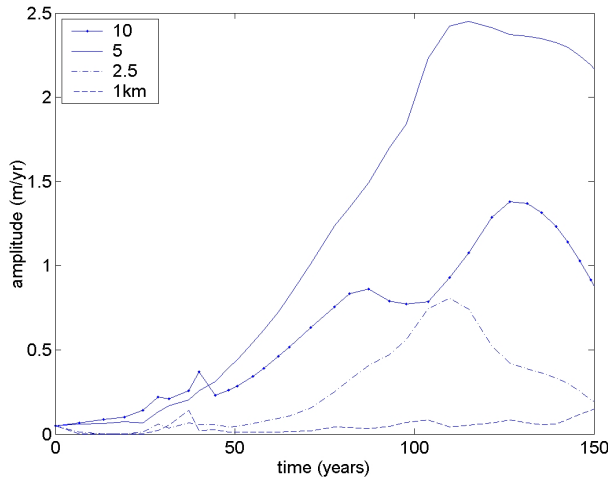


Figure 4. Amplitude of perturbation in 5 km wide basin during 150 years, around $x = 50$ km.

The development of a dominant wavelength that differs from the imposed perturbations suggests that the initial perturbation does not determine the final pattern. Two simulations with the narrow basin illustrate this. The bed of the basin is perturbed with alternating undulations of wavelength 1 km and 10 km, respectively. Independent of the initial perturbation, the dominant wavelength after 100 years is approximately 3 km in either case. Figure 5 shows that large-scale patterns may evolve from smaller-scale ones, but also that small-scale formations can develop on top of larger-scale initial patterns. Figure 6a presents the amplitude of the initially imposed λ_{10} and the developing smaller wavelengths during the simulated period for the section around $x = 65$ km. The growth of the imposed λ_{10} is smaller than that of the emerging smaller-scale modes. After 100 years the amplitude of smaller wavelengths exceeds the imposed perturbation. Additionally, Figure 6b shows the amplitudes in the basin with the initially imposed λ_1 . At the end of the simulation the same preference of wavelengths is observed as in Fig. 6a, but the amplitude of the most prevalent Fourier component with a wavelength of 3.3 km is larger. In Fig. 6a this component is still growing, while in Fig. 6b it is almost stabilised.

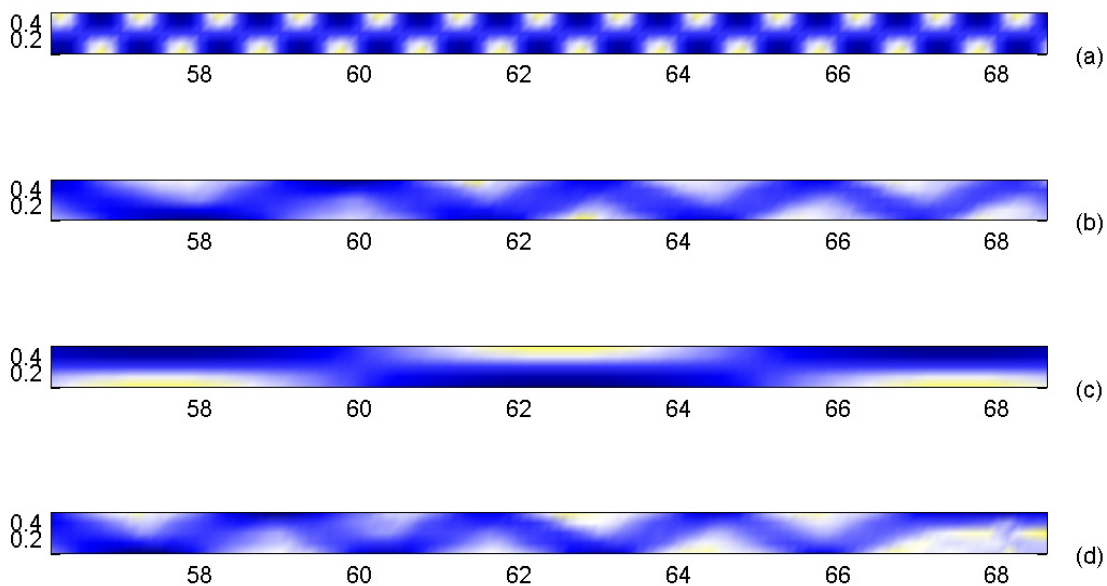


Figure 5. (a) Initial bottom perturbation λ_1 and (b) bathymetry after 100 year. (c) Initial bottom perturbation λ_{10} and (d) bathymetry after 100 year

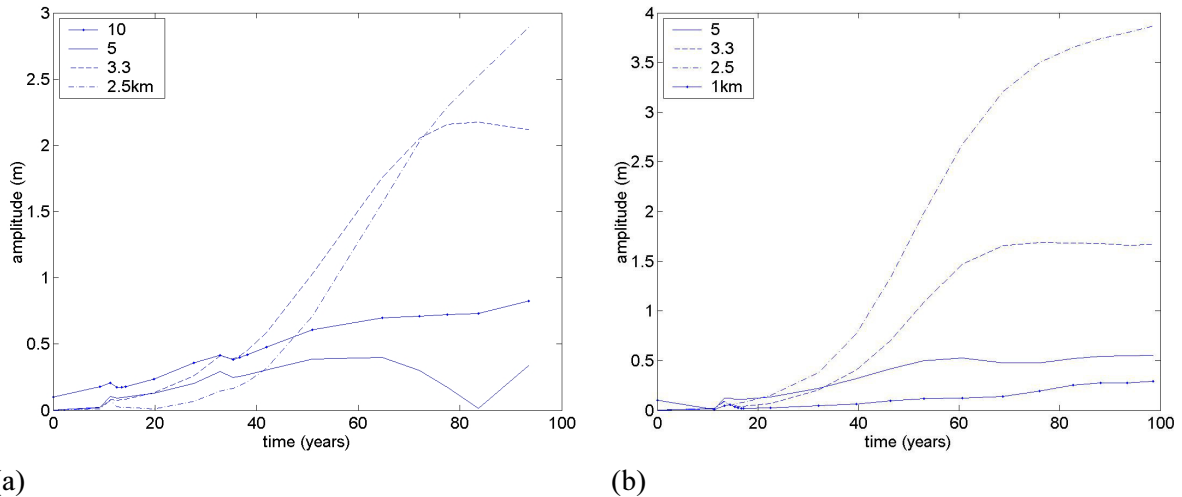


Figure 6. Amplitude of different meander wavelengths in a narrow basin (500 m), around km 65. An alternating pattern of (a) 10 km and (b) 1 km is imposed.

4 DISCUSSION

The simulations described in the foregoing show that evolved channel-shoal patterns have a dominant wavelength that depends on physical parameters like the width-to-depth ratio of the basin. This dependency is also observed in nature (Dalrymple and Rhodes, 1995). Another important result from the model is that this prevalent wavelength can change during the formation of the pattern. To increase the insight into the physical mechanisms and the observed dependency of preferred wavelengths on physical parameters, we can use results obtained with idealised models.

During the initial formation of the pattern, the amplitudes of the different perturbations grow exponentially. The period of exponential growth varies for the different perturbations. Figure 4 shows exponential growth of perturbation λ_{10} during 40 years and the growth of λ_5 can be regarded as exponential during 100 years. Also the amplitudes of damped perturbations decay exponentially. This is observed in Figure 7, for perturbation λ_1 in the narrow basin during the first 5 years. The exponential growth suggest that during this initial period the amplitudes are so small that the non-linear interaction of the perturbations can be neglected. Hence, the evolution can be described using a linear set of equations. This allows for a comparison between the initial results of the complex model and idealised models.

The model parameters and formulations in the idealised model of Schramkowski et al. (2002) are close to settings used in this process-based model. They find that the most unstable perturbation in a 5 km wide basin scales with the tidal excursion length, which is defined as the characteristic velocity divided by the tidal period. Quantitatively, it means that the preferred wavelength in the idealised model is about 7 km for a characteristic velocity in the basin of 1 m/s. In the complex model the prevalent wavelength is 10 km along the major part of the wide basin, which is close to this tidal excursion length. At the end of the basin the smaller perturbation λ_5 is more unstable. This can be explained by a decrease in the velocities (and therefore the tidal excursion length) near the landward end of the basin, which can be observed in Fig. 8. In the model of Schramkowski et al. the characteristic velocity is not varied. Another explanation is that for the small depths at the landward end, the friction

increases to values which are far from the critical value in the idealised model and not thoroughly described. In this domain other smaller perturbations can be more unstable. Besides agreement for the length scales of the prevalent perturbations, also the growth rates in both models are of the same order of magnitude. At present, a few model formulations still differ, which have to be adapted before further comparison can be made.

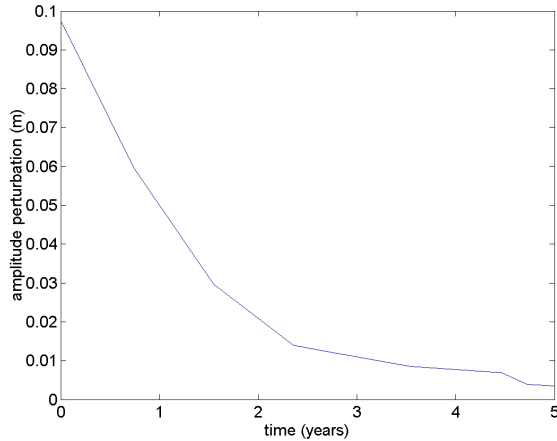


Figure 7. Exponential decay of perturbation λ_1 in small basin

In the narrow basin the velocities are equal to those in the wide basin. Therefore, the same prevalent wavelength is expected from the scaling parameter in the model of Schramkowski et al. However, in the complex model it is observed that the length scales are smaller than in the wide basin and the strong variation along the basin suggests dependence on the depth. From the study of Schramkowski et al. a slight dependency on the width can be concluded, but dependence on the depth is not investigated. Using another idealised model, Seminara and Tubino (2001) investigate the influence of the width-to-depth ratio on the prevalent wavelength. Their model results show that for an increasing width-to-depth ratio the wavenumber in longitudinal as well as in transversal direction increases, which implies a decrease in longitudinal meander wavelength for an alternating pattern. This is qualitatively in agreement with the results from the complex model.

The period of exponential growth of the perturbations during the long-term simulations indicate the application area of the idealised models. At a certain time, the amplitude ceases to adapt exponentially, after which the linearisation of the equations is no longer valid. Non-linear interactions determine the subsequent evolution of the pattern. The change in preferent wavelength as observed in Fig. 4 can be explained from these non-linear processes and therefore cannot be predicted by linearised models. Model results for this stage of pattern development can be validated against field data. Patterns resulting from the complex model and from field observations are shown to agree in Hibma et al. (2003a). A comparison of model results and observed empirical relationships between physical parameters and aggregated properties of the channel-shoal pattern is subject of further study.

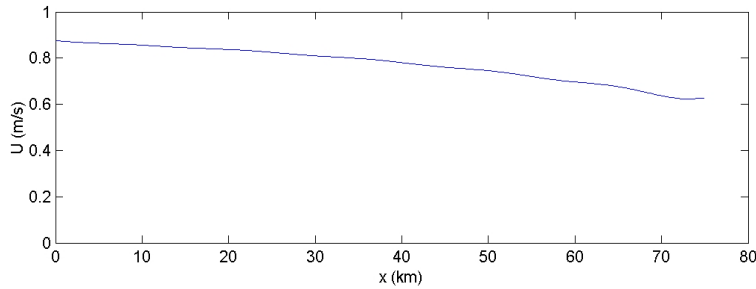


Figure 8. Amplitude of velocities along the basin.

5 CONCLUSION

A complex (process-based) model system was applied to simulate the formation of channels and shoals in an estuary. The estuary was schematised to a long ($L = 80$ km) rectangular basin. The initial bed topography was formed by a linear sloping bed on which sinusoidal perturbations of different wavelength were applied. The growth of channel-shoal patterns with different initial wavelengths was investigated and the dependency on the width and depth of the basin was studied. In order to increase the insight into the processes responsible for the channel-shoal formation, initial model results were compared to idealised models. Long-term simulations were made to investigate the effect of non-linear processes.

The results of the short-term model simulations show that the wavelength of the fastest growing perturbation increases for increasing depth and increasing width. In the wide estuary ($B = 5$ km) the most unstable wavelength of the imposed perturbations is 10 km in most of the basin. In the narrow estuary ($B = 500$ m) the preferent wavelengths are smaller and vary from 10 km at the deep seaward end to 2 km at the shallow landward end. This variation with the depth is larger than in the wide basin. The variations with width and depth are in agreement with the idealised model of Seminara and Tubino (2001). Comparison with the idealised model of Schramkowski et al. (2002) shows agreement for the growth rate and the preferred wavelength in the wide basin, which suggests that this wavelength scales with the tidal excursion length. This mutual validation of results from the idealised and complex models forms a step forward in the modelling of estuarine morphodynamics.

The growth curves during the long-term simulations over 100 to 150 years exhibit an exponential growth during the first decennia. During this period the linear approach of the idealised models is valid. The subsequent development of the channel-shoal pattern in the complex model can be attributed to non-linear processes. A long-term model run for the wide basin shows that the wavelength of the fastest growing mode changes from 10 km to 5 km during the simulation, due to this non-linear interaction. The long-term simulations show that modes with a wavelength different from the one of the imposed perturbations develop.

The minor changes in amplitude of the channel-shoal patterns at the end of the long-term simulations suggest that a morphodynamic equilibrium be reached. The wavelength of the pattern is independent of the initial perturbation. Similar to the initial formation, the dominant wavelengths seem to depend on the width and depth of the basin.

ACKNOWLEDGEMENT

The work presented herein was done in the framework of the DIOC-programme 'Hydraulic Engineering and Geohydrology' of Delft University of Technology, in theme 1 (Aggregated-scale prediction in morpho-dynamics), Project 1.4 (Intermediate-scale morphological behaviour of estuaries and coastal lagoons due to human interference). It is embedded as such in Project 03.01.03 (Coasts) of the Delft Cluster strategic research programme on the sustainable development of low-lying deltaic areas. This research was supported by NWO-ALW grant no. 810.63.12.

REFERENCES

- Dalrymple, R.W. and R.N. Rhodes (1995). Estuarine dunes and bars. In: *Geomorphology and sedimentology of estuaries* (Perillo, G.M.E., ed.). Elsevier, Amsterdam, 359-422.
- Coeveld, M., A. Hibma and M.J.F. Stive (2003). Feedback mechanisms in channel-shoal formation. Coastal Sediments Conference (published on CD).
- Hibma, A., H.J. de Vriend and M.J.F. Stive (2003a). Numerical modelling of shoal pattern formation in well-mixed elongated estuaries. *Estuarine and Coastal Shelf Science* (in press).
- Hibma, A., Schuttelaars H.M. & Wang Z.B. (2003b). Comparison of longitudinal equilibrium profiles of estuaries in idealized and process-based models. *Ocean Dynamics* (in press).
- Roelvink, J.A. and G.K.F.M. van Banning (1994). Design and development of DELFT3D and application to coastal morphodynamics. In: Babovic and Maksimovic (eds.), *Hydroinformatics*, Balkema, Rotterdam, p. 451-456.
- Schramkowski, G.P., H.M. Schuttelaars and H.E. de Swart (2002). The effect of geometry and bottom friction on local bed forms in a tidal embayment. *Continental Shelf research* 22, 1821-1833.
- Schuttelaars, H.M. and H.E. de Swart (1999). Initial formation of channels and shoals in a short tidal embayment. *J. Fluid Mech.*, vol.386, p. 15-42.
- Schuttelaars, H.M. and H.E. de Swart (2000). Multiple morphodynamic equilibria in tidal embayments. *Journal of Geophysical Research*, vol.105, no. C10, p. 24,105-24,118.
- Seminara, G. and M. Tubino (1998). On the formation of estuarine free bars. In: J. Dronkers and M. Scheffers (eds.), *Physics of estuaries and coastal seas*, Balkema, Rotterdam, p. 345-353.
- Seminara, G. and M. Tubino (2001). Sand bars in tidal channels. Part one: free bars. *J. Fluid Mech.* vol. 11.
- Vriend, H.J. de (1996). Mathematical modelling of meso-tidal barrier island coasts. Part I: Empirical and semi-empirical models. In: P.L.-F. Liu (ed.), *Advances in coastal and ocean engineering* (2), 115-149.
- Vriend, H.J. de and J.S. Ribberink (1996). Mathematical modelling of meso-tidal barrier island coasts. Part II: Process-based simulation models. In: P.L.-F. Liu (ed.), *Advances in coastal and ocean engineering* (2), 151-197.
- Wang, Z.B., H.J. de Vriend, and T. Louters (1991). A morphodynamic model for a tidal inlet, The Second International Conference on Computer Modelling in Ocean Engineering.
- Wang, Z.B., T. Louters and H.J. de Vriend (1995). Morphodynamic modelling of a tidal inlet in the Wadden Sea, *Journal of Marine Geology* 126 (1995) 289-300.